Effect of Molecular Weight on the Morphological Modifications Induced by UV Laser Ablation of Doped Polymers

Esther Rebollar,[†] Giannis Bounos,[‡] Mohamed Oujja,[†] Savas Georgiou,[‡] and Marta Castillejo*[,†]

Institute of Physical Chemistry Rocasolano, CSIC, Serrano 119, 28006 Madrid, Spain, and Foundation for Research and Technology-Hellas, Institute of Electronic Structure and Laser, P.O. Box 1527, 71110 Heraklion, Crete, Greece

Received: April 3, 2006; In Final Form: July 3, 2006

This work investigates the effect of polymer molecular weight (M_W) on the surface morphology of poly(methyl methacrylate) (PMMA) and polystyrene (PS) films doped with iodonaphthalene (NapI) and iodophenanthrene (PhenI) following irradiation in air at 248 nm. In agreement with previous studies, irradiation of PMMA at 248 nm results in surface swelling and bubble formation within the irradiated bulk. Most importantly, the size of bubbles varies sensitively for the different M_W values, with larger bubbles being formed for the low M_W systems. Nevertheless, the maximum swelling attains higher values for the high M_W values (when compared at the corresponding ablation threshold of the systems). Real-time monitoring of transmission of a probing beam shows that morphological changes last longer in the low M_W polymer. Melting, consistent with a thermal mechanism, occurs, and enough evidence is gathered to provide direct support for the bulk photothermal model, according to which ejection requires that a critical number of bonds is broken. In particular, the observed different morphological effects can be ascribed to the interplay of two factors, namely, of the much more efficient decomposition of the low M_W polymer to gaseous products and of the dependence of the mechanical polymer properties on M_W. For PS at 308 nm, the changes parallel the ones for PMMA at 248 nm. In contrast, at the strongly absorbed 248 nm, the morphological processes in PS show a less dramatic dependence on M_W. In all, these results are of direct importance for the optimization of laser processing schemes and applications (e.g., tissue processing, laser deposition, laser restoration, etc.).

1. Introduction

The molecular weight (M_W) of a polymer is an important parameter, as it determines many of its physical characteristics such as transition temperatures and mechanical properties.[1] In several laser processing schemes on real systems such as those encountered in medical and laser conservation applications, the M_W values of the treated polymeric-like substrates may vary a lot from case to case. Despite the fact that laser polymer ablation has been the subject of extensive research in the last 20 years,[2−5] only a few studies are available on the influence of M_W on the laser ablation of polymers.[6−11] Keely et al.[6] studied the effect of M_W on the 248 nm photoablation of polystyrene (PS) and observed little effect of this parameter on the etch rate. Ihlemann et al.[7] reported an influence of the degree of polymerization in their study about the ablation of doped poly(methyl methacrylate) (PMMA) at 308 nm. Masuhara et al.[8] have examined the temporal dynamics of the morphological changes of PMMA and PS of different M_W via time-resolved interferometry. They have shown that the time scale of expansion, and especially of contraction, of films upon laser irradiation differs for different M_W systems and have correlated this behavior with their different glass−rubber transition temperatures (T_g) and characteristic polymer chain lengths.

Recently,[9−11] we have reported initial results demonstrating the decisive influence of M_W on the morphological and chemical modifications induced in films of doped PMMA and PS upon UV laser irradiation. In this work, we present a comprehensive study on the morphological changes induced in different M_W systems. Films of PMMA, and PS, with average M_W's in the range 2−1000 kDa, were irradiated in air by a KrF excimer laser (248 nm, 20 ns fwhm) at fluences up to 2 J/cm^2 and by a XeCl excimer laser (308 nm, 30 ns fwhm) for selected experiments on PS-based films.

Morphological changes were established via optical and environmental scanning electron microscopy (ESEM) examination of the irradiated substrates. The temporal evolution of the modifications was monitored in situ and in real time via the attenuation of a CW probe HeNe laser by the irradiated film.

The results demonstrate a strong dependence of the extent and duration of the induced morphological changes on the polymer M_W as well as on the optical absorption coefficient at the irradiation wavelength of the polymer used. The implications derived for the mechanisms of polymer UV laser ablation are discussed. Furthermore, this sensitive dependence of processes on M_W occurring in a low absorbing polymer is of direct importance for the optimization of laser processing schemes and applications (e.g., tissue processing, laser deposition, laser restoration, etc.).

2. Experimental Section

Highly purified PMMA, with average M_W's of 2.5 kDa (Polymer Standard Services), 120 kDa, and 996 kDa (Aldrich), and PS, with average M_W's of 15.1 kDa (Polymer Standard Services), 280 kDa (Aldrich), and 532 kDa (Polymer Standard

* To whom correspondence should be addressed. Phone: +34-915619400. Fax: +34-915642431. E-mail: marta.castillejo@iqfr.csic.es.
† CSIC.
‡ Foundation for Research and Technology-Hellas.

10.1021/jp062060i CCC: $33.50
Published on Web 08/02/2006

TABLE 1: Swelling Onset and Ablation and Substrate Transmission Transient Thresholds (in mJ/cm^2), Optical Penetration Depth as Estimated from the Small-Signal Values (1/α) at 248 nm of Doped Polymer Films and Average Maximum Bubble Diameter after a Single Pulse (Errors Are Estimated in 10−20% for Determination of Thresholds and about 10% for Determination of Bubble Size)

system	M_W (kDa)	swelling	ablation	lowest fluence for detecting transmission transient	1/α (μm)	average maximum bubble diameter (μm)	maximum surface swelling (μm)
1.2% NapI/PMMA	2.5	250	1100	420	28	30	4
	120	600	1500	*a*		6	7
	996	650	1500	1200		5	8
0.5% PhenI/PMMA	2.5	200	500	*a*	18	21	*a*
	120	200	800−900	*a*		4	*a*
	996	300	1000	*a*		4	*a*
1.2% PhenI/PMMA	2.5	180	540	440	11	14	*a*
	120	180	800	*a*		5	*a*
	996	180	850	720		4	*a*
0.5% PhenI/PS	15.1	*b*	50	*b*	0.3	<0.5	*b*
	280	*b*		*b*		<0.5	*b*
	532	*b*		*b*		<0.5	*b*

[a] Not measured. [b] Not detectable.

Services), are doped with iodonaphthalene (NapI) and iodophenanthrene (PhenI) (Aldrich). Films are prepared by casting solutions of the purified polymer and of the dopant dissolved in dichloromethane (CH_2Cl_2) on quartz substrates. The dopant concentration varies from 0.5 to 1.2 wt %, and the typical film thickness is in the range 10−80 μm, as measured by a DEKTAK 3030 profilometer. Film absorption spectra have been measured on a Perkin-Elmer Lambda 16-UV/VIS spectrometer. The targets were irradiated in air by a KrF excimer laser (248 nm, 20 ns fwhm, 1 Hz) focused at normal incidence at fluences up to 2 J/cm^2. For selected experiments on PS-based films, irradiation was also carried out with a XeCl excimer laser (308 nm, 20 ns fwhm, 1 Hz).

Morphological changes of the irradiated films were established via optical microscopic examination by an optical Leica DM LM microscope and by environmental scanning electron microscopy (ESEM, Philips XL30). To measure the attenuation of a CW probe HeNe laser by the irradiated substrate, the laser was incident at 45° on the film, illuminating the area of the sample irradiated by the ablation laser with a matching size around 0.50 mm^2. The probe intensity was monitored in real time by a fast photodiode (response time 5 ns). A similar arrangement was used to monitor the attenuation of a second HeNe laser by the plume expanding in air, with the probe laser propagating in this case parallel to the irradiated surface at a given distance.

3. Results

3.1. Morphological Effects Induced on the Substrates. UV irradiation at 248 nm results in swelling and/or etching of PMMA films depending on the fluence. The ablation thresholds as determined by profilometry are collected in Table 1, which also lists the optical penetration depth (1/α) of the films calculated from the value of the linear absorption coefficient (α) directly measured on a UV−vis spectrometer.[10] For irradiation at weakly absorbed wavelengths, the swelling onsets and the etching thresholds increase with increasing M_W. However, at strongly absorbed wavelengths, the difference in the ablation thresholds is much smaller, or minimal.[10] Doping of PMMA results in an increase of the absorption coefficient which however is not dependent on the polymer M_W.[10] Below the threshold, swelling is observed for both NapI/PMMA- and PhenI/PMMA-doped systems although for the latter for concentrations higher than 0.5 wt % the elevation of the surface is barely measurable. When comparing at the corresponding ablation thresholds of 1.2% NapI/PMMA films, the maximum swelling is higher for the higher M_W system (Table 1).

Laser irradiated areas above swelling onsets display, under the optical microscope, morphological modifications depending on the irradiation wavelength and the optical absorption. Irradiation of PMMA films at 248 nm gives rise to the growth of microbubbles[9,10] (Figure 1). The typical bubble diameter, estimated by at least five different measurements, increases expectably with laser fluence until a maximum value is reached at a fluence slightly above the polymer ablation threshold (Table 1). This dependence can be ascribed to the higher amount of gaseous products accumulated in the substrate by the (photo)-thermal decomposition of the polymer with increasing laser fluence.[12] Once the ablation threshold is overcome, material starts to be ejected into the plume, thus limiting any further increase of bubble size. Figure 2 shows an example of the described behavior for films of 1.2% NapI/PMMA.

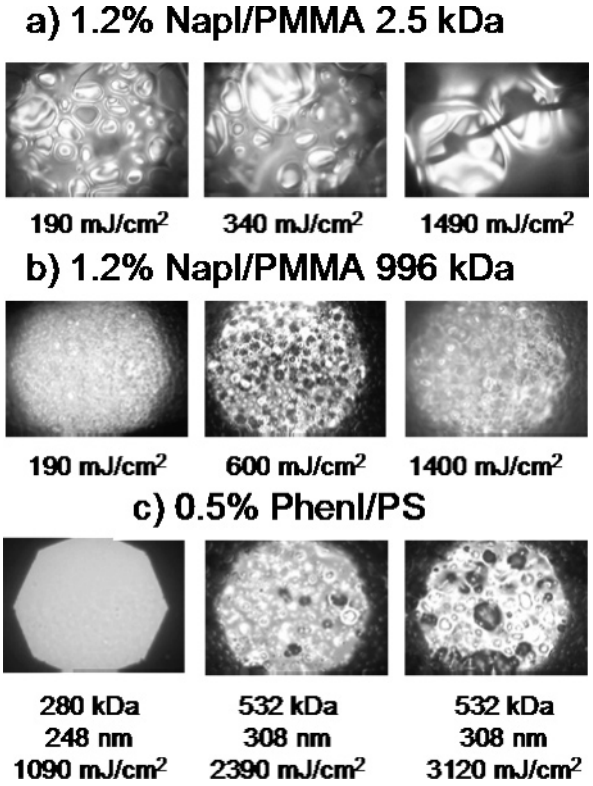

Figure 1. Optical micrographs (magnification 50×) of film areas irradiated with a single laser pulse at the indicated fluences: (a) 1.2% NapI/PMMA, 2.5 kDa, irradiated at 248 nm, (b) 1.2% NapI/PMMA, 996 kDa, irradiated at 248 nm, (c) 0.5% PhenI/PS irradiated at 248 and 308 nm. The size of each picture is 70 × 95 μm^2.

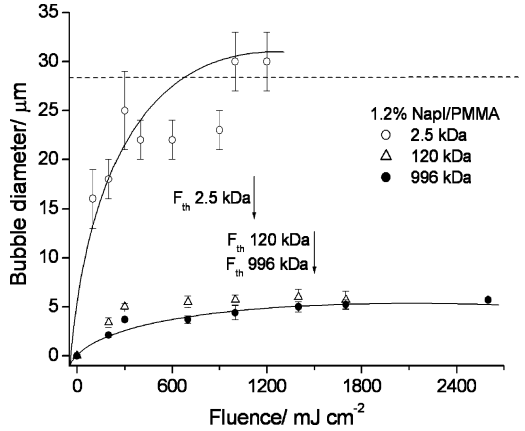

Figure 2. Bubble average diameter dependence as a function of fluence for samples of 1.2% NapI/PMMA, M_W = 2.5, 120, and 996 kDa, irradiated at 248 nm. The horizontal dashed line is drawn at the value (28 μm) of the optical penetration depth in the 2.5 kDa substrate. Continuous lines are visual guides. The ablation threshold fluences for the different M_W systems are indicated by arrows.

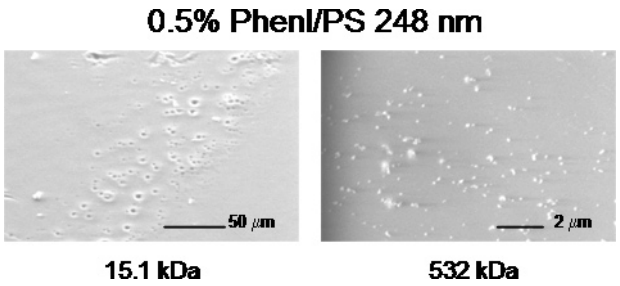

Figure 3. ESEM micrographs of 0.5% PhenI/PS, irradiated with a single pulse at 248 nm at 650 mJ/cm^2 with a polymer M_W of (a) 15.1 kDa and (b) 532 kDa.

Increasing the optical absorption coefficient through doping (e.g., $\alpha_{1.2NapI/PMMA}$ = 360 cm^{-1}, $\alpha_{0.5PhenI/PMMA}$ = 560 cm^{-1}, $\alpha_{1.2PhenI/PMMA}$ = 910 cm^{-1}) results in a decrease of the bubble size (Table 1). Following the same trend, upon irradiation of highly absorbing PS at 248 nm ($\alpha_{0.5PhenI/PS}$ = 3380 cm^{-1}), no swelling, bubbles, or other morphological modifications are visible under the optical microscope (Figure 1). Ablation at strongly absorbed wavelengths is induced without noticeable morphological modifications to the etched substrate ("clean etching"). In fact, as shown elsewhere by micro-Raman spectroscopy,[11] chemical modifications and degradation are negligible for the highly absorbing PS. On the other hand, irradiation of PS at 308 nm, where polymer absorption is low ($\alpha_{0.5PhenI/PS}$ = 340 cm^{-1}) induces micrometric size features in the substrate (Figures 1 and 3), in close similarity with the results obtained for PMMA at 248 nm. Although the decomposition pathways of PS may differ from those for PMMA, overall at comparable absorption coefficients, we find close correspondence between the two systems, as long as morphological changes are concerned. To investigate further the production of bubbles in the strongly absorbing substrates, samples of 0.5% PhenI/PS irradiated at 248 nm were observed with high resolution by ESEM. As seen in Figure 3, no morphological changes are detected in the irradiated area of the high M_W system, except for the presence of some redeposited material. However, in the low M_W system, bubbles with a diameter of few micrometers are visible.

Bubble formation and polymer surface swelling has been a common observation in ablation studies.[13−15] However, the dependence of M_W has not been examined. As demonstrated here, laser-induced morphological modifications, in particular

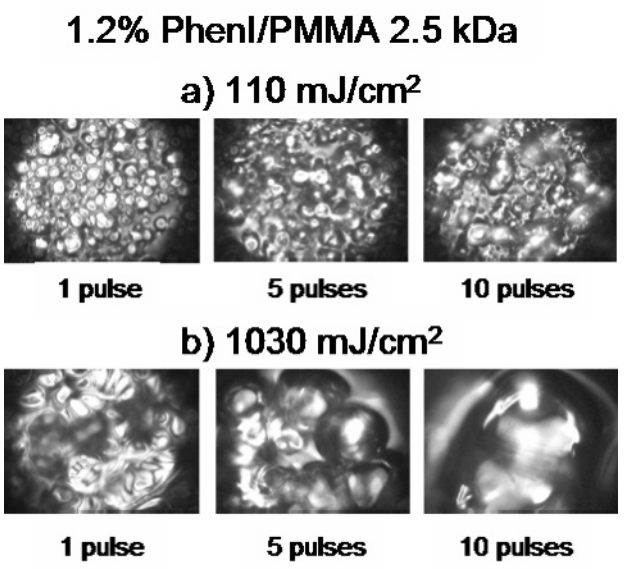

Figure 4. Optical micrographs (magnification 50×) of films of 1.2% PhenI/PMMA, 2.5 kDa, irradiated at 248 nm with the indicated fluences and number of pulses: (a) 110 mJ/cm^2, below ablation threshold; (b) 1030 mJ/cm^2, above ablation threshold. The size of each picture is 70 × 95 μm^2.

the size of the bubble, are observed to depend strongly on this polymer parameter. Bubbles are on average larger in the films of low M_W, this being a general behavior which is observed for systems with high and low linear absorption coefficients (α). Generally, the maximum bubble diameter is comparable to the optical penetration depth (1/α) (Figure 2). As this parameter does not change with M_W (experimentally checked), the differences in bubble size should be related to the M_W dependence on physical polymer properties, that is, the scaling up of glass transition temperature (T_g), viscosity, and tensile strength with M_W. Therefore, larger bubbles can grow in lower M_W polymer films that feature a larger available free volume and a lower viscosity.

To get more insight into the nature of the responsible mechanisms, the evolution of bubble size with the number of applied pulses was monitored. Figure 4 shows how bubbles increase in size with successive pulses (irradiation performed at a frequency of 1 Hz). The effect is observed at all fluences, but it is particularly noticeable above the ablation threshold. Irradiation at 1030 mJ/cm^2 of 1.2% PhenI/ PMMA, 2.5 kDa, with 5 and 10 pulses produces bubbles of 22 and 40 μm in diameter, respectively, much larger than the maximum value of 14 μm achieved by one-pulse irradiation (Table 1). This behavior is indicative of strong incubation effects which occur in materials with a low absorption coefficient at the laser wavelength.[15−18]

The incubation effects reported here are not related to heat accumulation induced by repetitive irradiation due to the slow repetition rate (1 Hz). The heat diffusion time in the targets can be estimated by $\tau_d \approx 1/(\alpha^2_{eff} D_{th})$, where α_{eff} is the effective absorption coefficient and D_{th} the thermal diffusivity ($\approx 11 \times 10^{-8}$ m^2/s for PMMA and similar for PS at 27 °C[19,20]). The effective absorption coefficients have been determined previously to be 1500−2000 cm^{-1} for 1.2% NapI/PMMA and larger for PhenI/PMMA and doped PS systems;[21] therefore, τ_d is estimated to be 0.2−0.4 ms for the former and somewhat shorter for the latter. These values are well below the interval between successive pulses, thus ensuring efficient heat dissipation prior to irradiation with the following laser pulse.

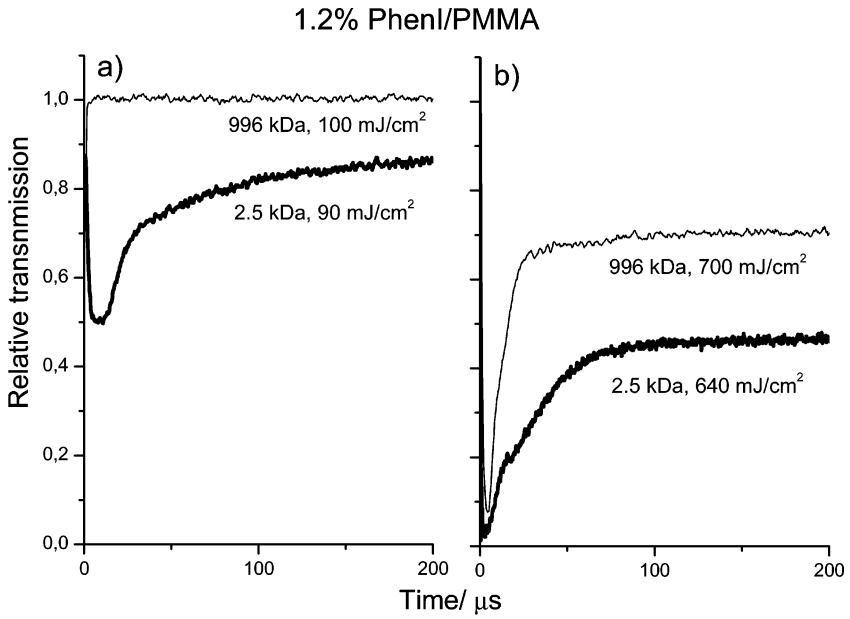

Figure 5. Time-resolved relative transmission of a CW HeNe laser by 1.2% PhenI/PMMA films irradiated at 248 nm with polymer M_W's of 2.5 kDa (thick line) and 996 kDa (thin line) at fluences (a) below ablation threshold and (b) above ablation threshold. The time origin represents the arrival of the 20 ns ablation pulse to the substrate.

Several authors have discussed the mechanisms of incubation in nanosecond UV irradiation of PMMA. Generally, incubation has been ascribed to the photoinduced formation of defect centers, that is, carbon double bonds at chain ends,[18] following backbone cleavage. The formation/accumulation of these products in the substrate increases the UV absorption and lowers the threshold, as well as the extent of decomposition resulting in further gas/bubble accumulation.

3.2. Substrate and Plume Transmission. The measurements of the real-time transmission of a CW laser through the irradiated film can provide information on the time scale of the morphological changes reported above. Figure 5 shows the transmission transients recorded by the photodiode in films of 1.2% PhenI/PMMA normalized to the initial transmission film value. Different transmission transients have been observed for systems of different M_W. For 2.5 kDa films, the transmission decreases sharply by as much as 50% within a few microseconds for a fluence below the ablation threshold (90 mJ/cm^2) and by nearly 100% for a fluence above threshold (640 mJ/cm^2). After the initial sudden reduction indicative of very fast bubble growth, the transmission recovers to a value that is lower than the initial one. In the high M_W polymer film, both the intensity and duration of the transmission transients are significantly reduced at the corresponding fluences. This is consistent with the results reported by Masubuchi[22] and Furutani[23] of a very fast expansion of the polymer surface upon irradiation, followed by a slow contraction. By using nanosecond time-resolved interferometry, these authors observed expansion and contraction of the surface at fluences below the swelling onset and eventually the recovery of the initial flat surface. On the contrary, at fluences above the swelling onset, expansion of the film was observed to start during the excitation laser pulse, followed by subsequent contraction, but in this case, the original flat surface was not recovered (i.e., swelling remained). The slow contraction corresponds roughly to the decay of the bubbles, as seen in Figure 5. This contraction can be ascribed to the decrease of the film temperatures, so that the production of gaseous species that drives bubble growth ceases, and also to the fact that, upon cooling, the viscosity and the rigidity of the polymer increases (resulting in bubble shrinkage).

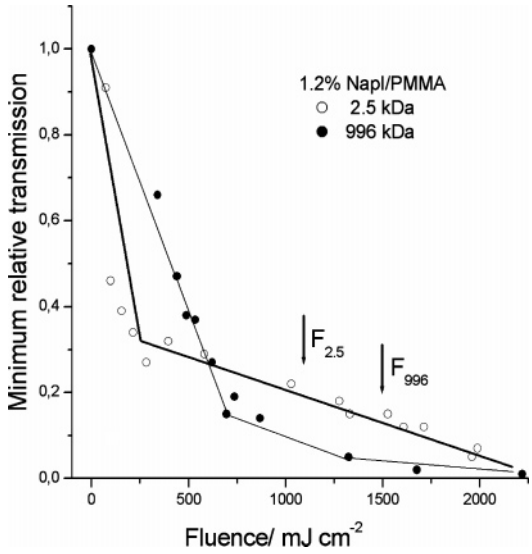

Figure 6. Fluence dependence of the minimum relative transmission of irradiated films (248 nm) of 1.2% NapI/PMMA of M_W = 2.5 kDa (open circles) and 996 kDa (full circles). The arrows indicate the ablation threshold of each sample. Lines are visual guides.

Figure 6 depicts the fluence dependence of the measured minimum relative transmission for 1.2% NapI/PMMA of 2.5 and 996 kDa. The fluence at which a significant reduction (of about 10%) of the transmission by the irradiated substrate is produced is slightly above the swelling onset of the films, and below the corresponding ablation threshold. The values of the threshold fluence for the appearance of the observed transmission transients are also listed in Table 1. Note that the decrease of the transmission at these fluences cannot be ascribed to scattering by material ejection. Indeed, simultaneous measurements of the transmission of a second CW HeNe laser propagating parallel to the substrate, and therefore probing exclusively the ablation plume, indicate that significant attenuation by the plume is only observed well above the ablation threshold of the films, when transmission by the substrate has already been severely reduced (Figure 7). These results indicate that the temporal scale of the substrate transmission transients

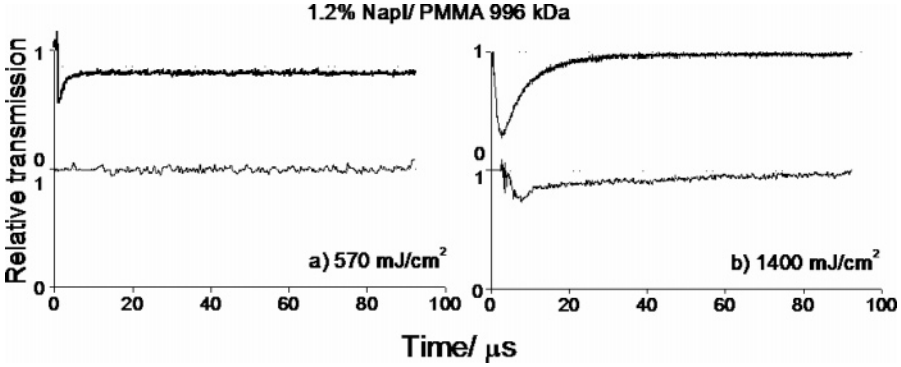

Figure 7. Time-resolved attenuation of the transmission of two HeNe CW lasers by the ablated substrate (thick upper line) and by the ablation plume at a distance of 200 μm from the surface (thin lower line) in 1.2% NapI/PMMA films irradiated at 248 nm at (a) 570 mJ/cm^2 and (b) 1400 mJ/cm^2.

reflects the evolution of the induced morphological modifications, that is, the time scale involved in the growth and decay of bubbles. The production of micron-sized bubbles results in a pronounced (Mie type) scattering of the probing beam. Given their very high number, especially at higher fluences, the probing beam most likely undergoes multiple scattering (changes in the refractive index of the material may also contribute partly to the probe beam attenuation).

In all, the transmission measurements reveal a slower decay of the size of bubbles produced by irradiation at 248 nm in the lower M_W PMMA films. Regarding highly absorbing PS-based films irradiated at 248 nm, neither the plume nor the substrate induces a significant attenuation of the probe beams, confirming the reduced extent of morphological modifications, as observed under the optical and ESE microscope. The difficulty in detecting scattering by the plume is mainly ascribed to the reduced amount of material that is ejected and to the fact that ejected material is mainly gaseous.[24]

4. Discussion

Morphological and chemical modifications induced by laser irradiation of weakly absorbing polymeric substrates have been reported by several authors.[13,14,25,26] However, their dependence on the polymer M_W value has been overlooked. Although the determining importance of the absorption coefficient to the extent of the morphological changes induced to the substrate has also been demonstrated here by the comparison of PS at 308 and 248 nm, the study shows that M_W is also an important factor for the extent of these changes.

Regarding the composition of the gaseous released material into the bubbles and in the ablation plume, previous studies on UV laser-induced ablation of PMMA have focused on the relative contribution of three different chemical processes:[3,5,27−32] (1) random homolytic scission of the polymer backbone, producing carbon radicals which can initiate unzipping reactions (depolymerization), (2) photolysis of the methyl side chain, producing chain end C═C double bonds and radicals, which can again initiate polymer unzipping, and (3) photolysis of the ester side group. As reported by several authors, photolysis of the ester side group often yields small radicals such as the methoxy, methyl, and methyl formate radicals[5,28,29] that can abstract hydrogen from the remainder of the polymeric chain. Hydrogen-atom abstraction from the polymer also produces main chain double bonds, which enhance laser absorption and provide sites for the initiation of thermal unzipping. A variety of experiments have confirmed that PMMA photolysis at wavelengths longer than 240 nm generates gaseous molecules (CH_3OH, CH_4, $HCOOCH_3$, CO, and CO_2), and that the associated chain radicals quickly react with small radicals or with other polymer chains.[5,30]

Results reported on the chemical changes effected in the systems of this work using Raman spectroscopy[11] indicate that, at irradiation fluences below the ablation threshold, the main effect induced in PMMA is the formation of the C═C bond as a consequence of the degradation of the polymer. For larger M_W systems, the larger increase of the corresponding Raman band demonstrates that polymer degradation is much more extensive for the higher M_W. Also, laser-induced fluorescence probing of the irradiated films[33] shows that, at fluences >250 mJ/cm^2, ArH formation (i.e., NapH and PhenH for NapI- and PhenI-doped PMMA, respectively) is increasingly higher in the high M_W system than in the low M_W system. Because ArH is formed via a simple thermal-activated reaction (i.e., hydrogen-atom abstraction from the polymer[34]), this result demonstrates that higher temperatures are attained in the high M_W PMMA. This finding directly also accounts for the higher extent of thermal decomposition of the polymer itself observed by the Raman results. The higher extent of decomposition for the high M_W is also demonstrated by the fact that, below ablation threshold, though swelling is observed for the poorly absorbing systems, it is much more pronounced for the higher M_W system (Table 1).

Thermal unzipping of PMMA leads to efficient momomer (MMA) production, while random chain scission is responsible for higher mass fragments (oligomers). In the case of the doped systems actually studied here, the thermal decomposition/unzipping process dominates.[34,35] The efficiency of monomer production (pre-exponential Arrhenius factor and activation energy for degradation) as well as the efficiency of the photolysis of the side groups show little dependence on M_W. Thus, the gaseous composition within the bubbles is not expected to differ much between the different M_W's. Already at low enough fluences ($\geq$200 mJ/cm^2), high enough temperatures are developed at relatively low fluences, as a result of the increasing importance of nonlinear/multiphoton absorption processes. Multiphoton processes have been demonstrated in the irradiation at 248 nm of PMMA with a variety of dopants.[23,36,37] Since the absorption coefficient is independent of the PMMA M_W, a direct photolytic process cannot explain why polymer decomposition should vary with M_W. Instead, as discussed below, the thermal decomposition process can rather directly account for this dependence. In view of the above, the different morphological processes/effects that have been observed are mainly determined by the above temperature differences and by the intrinsic mechanical properties of PMMA.

Several mechanisms have been proposed to describe UV laser ablation of polymers. For ablation of PMMA at 248 nm, a

photothermal mechanism is strongly suggested,[9−12] where material ejection involves thermal decomposition of the polymeric chains to oligomers or monomers that subsequently desorb. In the so-called bulk photothermal model,[26,38] material ejection starts once the polymer fragments reach a small enough size to desorb/be ejected into the plume. The results presented here are consistent with this mechanism, which provides a framework for explaining the dependence on polymer M_W. Accordingly, more laser energy has to be coupled into the substrate to produce, from an initially longer polymer chain, fragments able to desorb, thus explaining the higher ablation threshold of the higher M_W PMMA substrates. Indeed, as we describe elsewhere,[33] modeling of the kinetics of the laser-induced processes directly shows that much higher temperatures are attained by the high M_W polymers. At the corresponding ablation thresholds, a temperature of ~600 K is estimated for the low M_W PMMA, whereas the temperature is ~850 K for $M_W > 120$ kDa. This is easily understood by the highly efficient decomposition of the low M_W systems to small oligomers and monomers, which therefore result in efficient energy removal from the system via their desorption. As a result of the higher temperatures, thermal decomposition of the high M_W PMMA is considerably higher, as indeed confirmed by Raman spectroscopic examination.[11]

Bubble formation and aggregation following irradiation with successive pulses are indicative of a volume heating of the substrate. The transient drop of the substrate transmission, as measured in this work for PMMA-based films, should be ascribed to the enhanced scattering and refraction of the probing beam by the gaseous bubbles formed in the film.[39] The lower viscosity of this substrate facilitates the diffusion of gaseous products within the heated volume and the growth of larger bubbles. The time scale in which these effects contribute to the observed transmission changes of the irradiated substrate can thus be correlated with the time scale of bubble growth. On the other hand, attenuation of the beam probing the plume is due to scattering and absorption by species ejected from the substrate.[40]

Bubble growth within viscoelastic materials, such as polymer melts, is a highly complex issue. In the case of laser irradiation, the quantitative description is further hindered by the fact that polymer properties (e.g., viscosity, etc.) vary much with time, depending on the temporal evolution of the attained film temperatures and of the extent of decomposition. Nevertheless, a qualitative description can account for the observations in a satisfactory way. The expansion of bubbles in a viscous liquid[41] is given by

$$R\frac{d^2R}{dt^2} + \frac{3}{2}\left(\frac{dR}{dt}\right)^2 = \frac{1}{\rho}(P_g(t) - P_0) - 4\frac{\eta}{R}\frac{dR}{dt} - \frac{2\sigma}{\rho R} - f(\text{Elastic}) \quad (1)$$

where R denotes the bubble radius, η the viscosity, P_g the time-dependent pressure of gas accumulated within the bubbles, P_0 the ambient (external) pressure, σ the surface tension, and ρ the density and f(Elastic) represents the term required for the viscoelastic deformation of the polymer. Thus, the rate of bubble growth increases with decreasing η.

It would appear that, for high M_W systems, the very high η value[42]

$$\log \eta = \log \eta_{cr} + 3.4 \log M_W/M_{W\,cr} \quad (2)$$

where η_{cr} is the viscosity at the entanglement point (~30 kDa for PMMA) could severely limit bubble growth. However, as shown elsewhere,[33] much higher temperatures are attained at high M_w and their thermal decomposition is much more extensive. As a result, η is much reduced, and thus, bubble formation is more efficient than expected from literature values.

TABLE 2: Glass Transition Temperature (T_g) of PMMA and PS of Different Molecular Weights Calculated According to the Flory−Fox Equation[43] (See Text)

polymer	M_W (kDa)	T_g (°C)
PMMA	1.9	26
	2.5	47
	120	110
	996	111
PS	15.1	89
	280	99
	532	100

Both the higher rate of formation of gaseous species (oligomers, monomers), that is, resulting in a higher P_g value within the bubbles, and the lower σ, η, and f(Elastic) values for the low M_W melt contribute to produce larger and faster bubble growth for the low M_W systems. In fact, a further factor promoting bubble formation at low M_W, and which is not included in the simplified formula (eq 1), includes the much higher diffusion of gaseous products. Because of the dependence of polymer σ and η on M_W, a correspondence between the observed bubble sizes and the glass transition temperatures may be expected. Indeed, the dependence of the size of bubbles on M_W closely follows the dependence of the mentioned polymer properties with this parameter. In the case of T_g, this dependence can be modeled by the Flory−Fox equation[43]

$$T_g = T_{g,\infty} - \frac{K}{X_n} \quad (3)$$

where $T_{g,\infty}$ is the asymptotic value at high M_W, K is a constant which depends on the polymer ($K = 1607$ and 1635 for PMMA and PS, respectively[43,44]), and X_n is the monomer number ($X_n = M_W/M_0$, where M_0 is the monomer molecular weight). Values of T_g for PMMA and PS at the different M_W values used in this work are listed in Table 2. The corresponding values in the doped polymers could differ slightly from the ones listed due to the plastizicing effect of the dopant.[45] However, as the dopant concentration is very low (ranges from 0.5 to 1.2 wt %), its effect on T_g should be minimal. Therefore, larger bubbles can grow in lower M_W polymer films that feature a larger available free volume and a lower viscosity. In addition, because of the lower opposing f(Elastic) value, bubbles should decay slower at low M_W, as indeed is observed in the transmission experiments.

In view of the above conclusion, it is important to notice that the maximum polymer surface swelling (measured profilometrically) just below the corresponding ablation thresholds is much higher for the higher M_W's. Considering the much higher elastic constant, the higher swelling of the high M_W PMMA clearly shows that a much higher amount of gaseous products must be accumulated/formed in the substrate for material ejection to occur. This affords a strong indication for the operation of the bulk photothermal model.

Lower ablation thresholds are obtained for the PS-based systems in correspondence with the higher absorption coefficient of this polymer (more than 30 times), as compared with PMMA. Bubbles are not detected because their size is limited within the submicron heated depth (i.e., the very small optical penetration) close or below the limits of optical detection. In

addition, likely, desorption of gases from the free surface becomes more likely, thus limiting their accumulation within bubbles.

5. Conclusions

Demonstration for a strong influence of polymer M_W on the extent and time evolution of morphological changes induced by UV laser irradiation on low absorbing polymer films has been presented. In all, both higher gaseous production and the mechanical polymer properties promote bubble formation in the low M_W PMMA. Furthermore, the observation of higher ablation thresholds as well as of higher surface swelling for the high M_W PMMA can be well explained by invoking the bulk photothermal model according to which a necessary condition for ablation is the cleavage of a critical number of bonds.

Acknowledgment. Work funded by Spanish Project MCYT BQU2003-08531-C02-01. E.R. and M.C. thank the Ultraviolet Laser Facility operating at FO.R.T.H. under the Improving Human Potential (IHP)-Access to Research Infrastructures program (RII3-CT-2003-506350). E.R. and G.B. thank support by the ESF COST Action G7. Support by PENED 01EΔ419 administered by the Greek Ministry of Development is acknowledged. M.O. and E.R. acknowledge CSIC I3P for a contract and a fellowship, respectively. Thanks are given to D. Gómez-Varga for the ESEM micrographs.

References and Notes

(1) Van Krevelen, D. W. *Properties of Polymers*; Elsevier Science B. V: Amsterdam, The Netherlands, 1990.
(2) Srinivasan R.; Braren, B. *Chem. Rev.* **1989**, *89*, 1303.
(3) Lippert, T,; Dickinson, J. T. *Chem. Rev.* **2003**, *103*, 453.
(4) Georgiou, S. *Adv. Polym. Sci.* **2004**, *168*, 1.
(5) Lippert, T.; Webb, R. L.; Langford, S. C.; Dickinson, J. T. *J. Appl. Phys.* **1999**, *85*, 1838.
(6) Lemoine, P.; Blau, W.; Drury, A.; Keely, C. *Polymer* **1993**, *34*, 5028.
(7) Lippert, T.; Wokaun, A.; Stebani, J.; Nuyken, O.; Ihlemann, J. *D. Angew. Makromol. Chem.* **1993**, *213*, 127.
(8) Mito, T.; Masuhara, H. *Appl. Surf. Sci.* **2002**, *197*−*198*, 796.
(9) Rebollar, E.; Bounos, G.; Oujja, M.; Domingo, C.; Georgiou, S.; Castillejo, M. *Appl. Surf. Sci.* **2005**, *248*, 254.
(10) Rebollar, E.; Bounos, G.; Oujja, M.; Georgiou, S.; Castillejo, M. *J. Phys.: Conf. Ser.*, in press.
(11) Rebollar, E.; Bounos, G.; Oujja, M.; Domingo, C.; Georgiou, S.; Castillejo, M. *J. Phys. Chem. B*, **2006**, *110*, 14215.
(12) Rebollar, E.; Oujja, M.; Castillejo, M.; Georgiou, S. *Appl. Phys. A* **2004**, *79*, 1357.
(13) Efthimiopoulos, T.; Ciagias, Ch.; Heliotis, G.; Heliodonis, E. *Can. J. Phys.* **2000**, *78*, 509.
(14) Lazare, S.; Tokarev, V.; Sionkowska, A.; Wisniewski, M. *Appl. Phys. A* **2005**, *81*, 465.
(15) Srinivasan, R.; Braren, B.; Casey, K. G.; Yeh, M. *J. Appl. Phys.* **1990**, *68*, 1842.
(16) Küper, S.; Stuke, M. *Appl. Phys. A* **1989**, *49*, 211.
(17) Krajnovich D. J. *J. Phys. Chem. A* **1997**, *101*, 2033.
(18) Blanchet, G. C.; Cotts, P.; Fincher, C. R., Jr. *J. Appl. Phys.* **2000**, *88*, 2975.
(19) Bäuerle, D. *Laser Processing and Chemistry*; Springer-Verlag: Berlin, Heidelberg, 2000.
(20) Touloukian, Y. S.; Powell, R. W.; Ho, C. Y.; Nicolaou M. C. *Thermal Diffusivity*; Thermophysical Properties of Matter, Vol. 10; IFI/Plenium: New York, 1973.
(21) Bounos, G.; Athanassiou, A.; Anglos, D.; Georgiou, S. *Chem. Phys. Lett.* **2006**, *418*, 317.
(22) Masubuchi, T.; Furutani, F.; Fukumura, H.; Masuhara, H. *J. Phys. Chem. B* **2001**, *105*, 2518.
(23) Furutani, H.; Fukumura, H.; Masuhara, H. *J. Phys. Chem.* **1996**, *100*, 6871.
(24) Rebollar, E.; Gaspard, S.; Oujja, M.; Villavieja, M. M.; Corrales, T.; Bosch, P.; Georgiou, S.; Castillejo, M. *Appl. Phys. A* **2006**, *84*, 171.
(25) Srinivasan, R.; Braren, B.; Casey, K. G. *Pure Appl. Chem.* **1990**, *62*, 1581.
(26) Bityurin, N.; Luk'yanchuk, B. S.; Hong, M. H.; Chong, C. T. *Chem. Rev.* **2003**, *103*, 519.
(27) Beauvois, S.; Renaut, D.; Lazzaroni, R.; Laude, L. D.; Bredas, J. G. L. *Appl. Surf. Sci.* **1997**, *109*−*110*, 218.
(28) Wochnowski, C.; Shams-el-Din, M. A.; Metev, S. *Polym. Degrad. Stab.* **2005**, *89*, 252.
(29) Shams-el-Din, M. A.; Wochnowski, C.; Metev, S.; Hamza, A. A.; Jüptner, W. *Appl. Surf. Sci.* **2004**, *236*, 31.
(30) Gupta, A.; Liang, R.; Tsay, F. D.; Moacanin, J. *Macromolecules* **1980**, *13*, 1696.
(31) Dijkkamp, D.; Gozdz, A. S.; Venkatesan, T.; Wu, X. D. *Phys. Rev. Lett.* **1988**, *60*, 381.
(32) Blanchet, G. *Macromolecules* **1995**, *28*, 4603.
(33) Bounos, G.; Rebollar, E.; Selimis, A.; Bityurin, N.; Castillejo, M.; Georgiou, S. *J. Appl. Phys.*, in press.
(34) Bounos, G.; Kolloch, A.; Stergiannakos, T.; Varatsikou, E.; Georgiou, S. *J. Appl. Phys.* **2005**, *98*, 1.
(35) Manring, L. E. *Macromolecules* **1991**, *24*, 3304.
(36) Fukumura, H.; Masuhara, H. *Chem. Phys. Lett.* **1994**, *221*, 373.
(37) Fujiwara, H.; Nakajima, Y.; Fukumura, H.; Masuhara, H. *J. Phys. Chem.* **1995**, *99*, 11481.
(38) Arnold, N.; Bityurin, N. *Appl. Phys. A* **1999**, *68*, 615.
(39) Baudach, S.; Bonse, J.; Krüger, J.; Kautek, W. *Appl. Surf. Sci.* **2005**, *154*−*155*, 254.
(40) Kukreja, L. M.; Hess, P. *Appl. Surf. Sci.* **1994**, *79*−*80*, 158.
(41) Brennen, C. E. *Cavitation and Bubble Dynamics*; Oxford University Press: New York, 1995.
(42) Colby, R. H.; Fetters, L. J.; Graessley, W. W. *Macromolecules* **1987**, *20*, 2226.
(43) Fox, T. G., Jr.; Flory, P. J. *J. Appl. Phys.* **1950**, *21*, 581.
(44) O'Driscoll, K.; Amin, Sanayei, R. *Macromolecules* **1991**, *24*, 4479.
(45) Wang, C. H.; Xia, J. L. *J. Chem. Phys.* **1990**, *92*, 2603.